European Commission

JRC TECHNICAL REPORTS

PESETA III – Task1: Climate change projections, bias-adjustment, and selection of model runs

Dosio, A.

2018

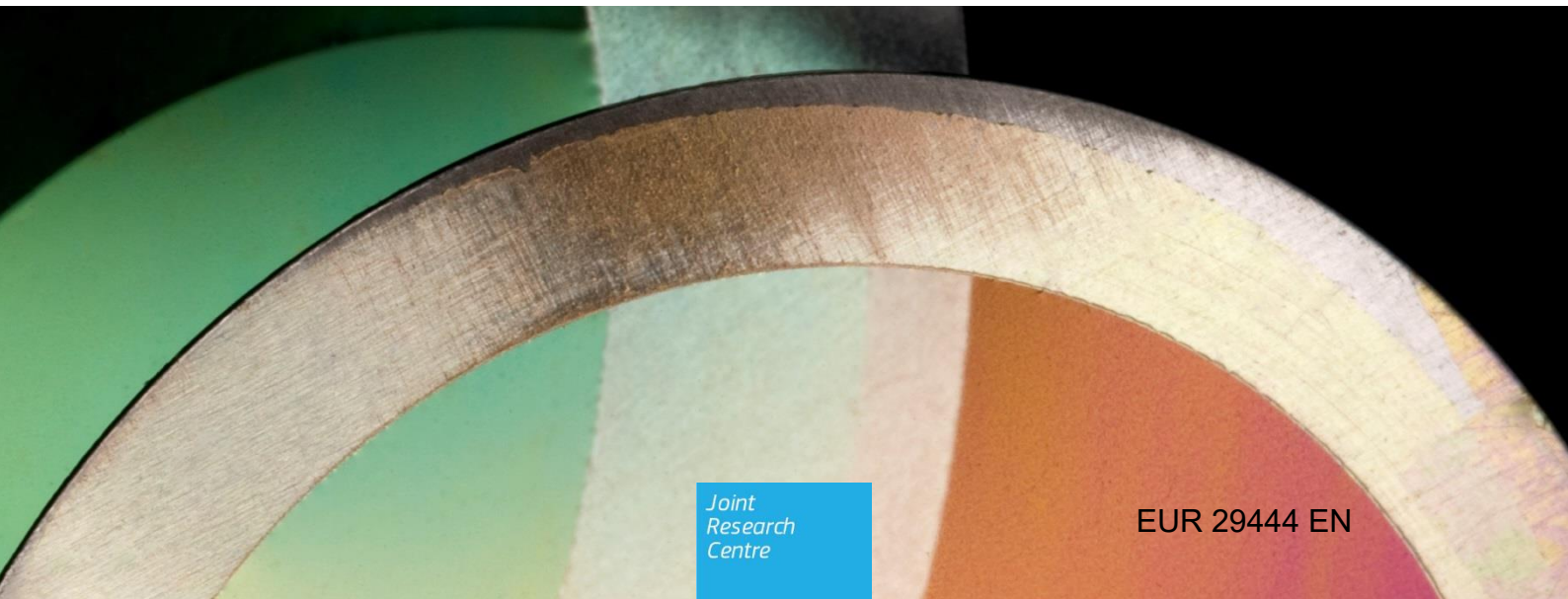

Joint Research Centre

EUR 29444 EN

Contact information
Name: Alessandro Dosio
Address:
Email: alessandro.dosio@ec.europa.eu
Tel.: +390332786626

JRC Science Hub
https://ec.europa.eu/jrc

JRC113745

EUR 29444 EN

ISBN 978-92-79-97261-4, ISSN 1831-9424, doi:10.2760/44883

Luxembourg: Publications Office of the European Union, 2018

How to cite this report: Dosio A., 2018. *PESETA III* – Task 1: Climate change projections, bias-adjustment, and selection of model runs. EUR 29444-EN, doi:10.2760/44883

Contents

Acknowledgements

The bias correction code used here was originally developed under the European Union FP6 integrated Project WATCH (contract 036946) by C. Piani and J.O.Haerted, who kindly provided the bias correction code.

The EURO-CORDEX data used in this work were obtained from the Earth System Grid Federation server (https://esgf-data.dkrz.de/projects/ esgf-dkrz/). We are grateful to all the modeling groups that performed the simulations and made their data avail- able, namely, Laboratoire des Sciences du Climat et de l'Environnement (IPSL), Institut National de l'Environnement Industriel et des Risques, Verneuil en Halatte (INERIS), the CLM community (CLMcom), the Danish Meteorological Institute (DMI), the Royal Netherlands Meteorological Institute (KNMI), and the Rossby Centre, Swedish Meteorological and Hydrological Institute (SMHI).

Authors

Alessandro Dosio (alessandro.dosio@ec.europa.eu)

Executive summary

Global warming will greatly affect the climate at regional and local scale through, e.g., the increase of intensity and frequency of extreme weather events (floods, droughts, heat waves, etc.). In order to assess the impact of climate change at such scale (on, e.g., the hydrological cycle or crop production) it is necessary to attain meteorological information with a spatial detail much finer than that provided by global climate models (GCMs). High-resolution climate projections are usually obtained by employing regional climate models (RCMs), which are able to better resolve small-scale features such as topography and heterogeneous land use.

When compared to present-day observations, however, the results of climate models can present large biases; in order to be used as an input for process-based impact models (like in PESETA III) outputs from RCMs are usually further post-processed by means of statistical techniques known as bias-correction (or bias-adjustment).

Here, we describe the projections of climate change used in PESETA III and the bias-adjustment method applied to them, focusing on the analysis of a series of climate change indices for both the mean climate and extreme events (such as the number of frost days, of the number of consecutive dry days) relevant for impact assessment studies.

Results show that, under the RCP8.5 emission scenario, at the end of the Century, maximum temperature is expected to increase, in winter, between about 2.5◦C over the British Isles and 4.8◦C over Scandinavia. In summer, the projected change ranges between 2.5◦C over Britain and 4.7◦C over the Iberian Peninsula.

Winter precipitation is projected to increase over most of central and northern Europe in both frequency, and intensity, with a consequent increase of the number of consecutive wet days, and reduction of consecutive dry days. The change in precipitation frequencies distribution is not uniform, though, and a reduction in low precipitation intensity is accompanied by an increase of extreme events, even for the Mediterranean regions where total precipitation is projected to decrease. In summer, a general reduction in precipitation is projected for all regions except Scandinavia and Eastern Europe; as for winter, there is a tendency toward less frequent but more severe precipitation episodes.

A set of 12 RCMs' bias-adjusted climate change projections is provided to the PESETA III impact modellers; the use of such a large ensemble of runs is essential to quantify the uncertainty in climate projections (the so-called inter-model variability). In fact, each model's run (driven by the same emission scenario) represents an equally plausible projection of the future evolution of the climate. However, due to differences in the models' formulation and physical parameterization, the climate change signal projected by different models may present significant differences.

Due to resource limitations, some impact model groups may not be able to use all the 12 provided runs; in this case, a sub-set of 5 runs is selected to be used by all impact models (compulsory core runs). The sub-set of core runs needs to be able to reproduce, as accurately as possible, the inter-model variability of the entire ensemble. The selection of the sub-set has been performed by means of Principal Component Analysis (PCA) on the bias adjusted climate change indices.

Finally, the PESETA III protocol also requires investigating the impacts of a 2°C global warming, compared to the preindustrial period. Here for each RCM run, the timing of reaching 2°C warming is provided following the same procedure used in the FP7 project IMPACT2C, namely:

- It is assumed that the climate in a +2°C world is comparable irrespective of when and how fast this warming is reached
- An RCM is defined to project a 2°C global warming when the corresponding driving GCM reaches the 2°C threshold, under RCP8.5 emission scenario
- For each GCM-RCM run, the +2°C period is defined as the 30 year period centred around the year when the 2°C global warming is first reached

1 Introduction

To obtain climate change information suitable for local–scale impact assessment (e.g. river flood or crop production), the output from global climate models (GCMS, whose spatial resolution may be too coarse) is further downscaled by employing high-resolution regional climate models (RCMs.), which are able to better resolve small-scale features such as topography and heterogeneous land use. However, the resulting downscaled climate information may still present large errors, when compared to present-day observations; these errors are inherited from the driving GCM, in addition to those introduced by the RCM by means, for instance, of model errors and parametrizations (e.g. Fowler et al., 2007).

These intensity-dependent biases can have a large impact not only on the model's representation of the present-day climate, but also on its future projection (Dosio et al., 2012; Maurer and Pierce, 2014; Mbaye et al., 2015).

Before being used as an input for process-based impact models, therefore, outputs from climate models are usually further post-processed to reduce their biases ((Piani et al., 2010a; Li et al., 2010; Themeßl et al., 2011; Thrasher et al., 2012; Ehret et al., 2012). Among several techniques, statistical bias correction (or bias-adjustment) is increasingly used in studies of assessment of the impact of climate change on several sectors including floods, agriculture, and forest fires (Rojas et al., 2011; Migliavacca et al., 2013; Russo et al., 2013; Ruiz-Ramos et al., 2015 Gabaldón-Leal et al., 2015).

However, it is important to note that, as bias-adjustment affects directly the probability distribution function of the climate variable, both in the present and future, the bias-adjusted climate, and, in particular, the probability of extreme events under climate change, can differ from the original (i.e., non bias-adjusted) one.

Here, we discuss the methodology to provide PESETA III impact modellers with high resolution, bias-adjusted projections of climate change. In particular, three main topics are discussed:

1) the bias-adjustment technique and its effect of a number of climate change indices for the mean climate change signal and extreme events, which are relevant for impact assessment on different sectors
2) a methodology based on Principal Component Analysis (PCA) in order to select a subset of models' runs to be used as core runs (i.e. compulsory to all participant impact groups) in PESTEA III
3) a methodology to identify the timing of reaching a 2°C global warming compared to preindustrial period, to investigate the impact, at European level, of a +2°C world.

2 Data and methods

2.1 Regional Climate Models

Modelled temperature and precipitation daily data are obtained from an ensemble of RCMs participating to the Coordinated Regional-climate Downscaling Experiment over Europe (EURO-CORDEX, http://www.cordex.org/) (e.g., Jacob et al., 2013). RCMs were used to downscale the results of GCMs participating to the Coupled Model Intercomparison Project Phase 5 (CMIP5; Taylor et al. 2012) over a numerical domain covering the entire European continent at a resolution of 0.11° (around 12 Km). Historical runs, forced by observed natural and anthropogenic atmospheric composition, cover the period from 1950 to 2005, whereas the projections (2006–2100) are forced by Representative Concentration Pathway RCP8.5 (Vuuren et al., 2011). RCP8.5 (i.e., with a radiative forcing value of +8.5 W/m^2) combines assumptions about high population and relatively slow income growth with modest rates of technological change and energy intensity improvements, leading in the long term to high energy demand and GHG emissions in absence of climate change policies. RCP8.5 thus corresponds to the pathway with the highest greenhouse gas emissions, without any specific climate mitigation target.

The full list of models' runs is reported in Table 1.

Table 1. List of models' runs used in PESETA III

Institute	RCM (R)	Driving GCM (G)	CORDEX full name	Acronym (R-G)
CLMcom	CCLM4.8-17	CNRM-CERFACS-CNRM-CM5	CNRM-CERFACS-CNRM-CM5_r1i1p1_CLMcom-CCLM4-8-17	R1-G1
		ICHEC-EC-EARTH	ICHEC-EC-EARTH_r12i1p1_CLMcom-CCLM4-8-17	R1-G2
		MPI-M-MPI-ESM-LR	MPI-M-MPI-ESM-LR_r1i1p1_CLMcom-CCLM4-8-17	R1-G3
DMI	HIRHAM5	ICHEC-EC-EARTH	ICHEC-EC-EARTH_r3i1p1_DMI-HIRHAM5	R2-G2
IPSL-INERIS	WRF331F	IPSL-IPSL-CM5A-MR	IPSL-IPSL-CM5A-MR_r1i1p1_IPSL-INERIS-WRF331F	R3-G4
KNMI	RACMO22E	ICHEC-EC-EARTH	ICHEC-EC-EARTH_r1i1p1_KNMI-RACMO22E	R4-G2
SMHI	RCA4	CNRM-CERFACS-CNRM-CM5	CNRM-CERFACS-CNRM-CM5_r1i1p1_SMHI-RCA4	R5-G1
		ICHEC-EC-EARTH	ICHEC-EC-EARTH_r12i1p1_SMHI-RCA4	R5-G2
		IPSL-IPSL-CM5A-MR	IPSL-IPSL-CM5A-MR_r1i1p1_SMHI-RCA4	R5-G4
		MOHC-HadGEM2-ES	MOHC-HadGEM2-ES_r1i1p1_SMHI-RCA4	R5-G5
		MPI-M-MPI-ESM-LR	MPI-M-MPI-ESM-LR_r1i1p1_SMHI-RCA4	R5-G3

2.2 Bias-adjustment of climate projections

The bias-adjustment technique, originally developed by Piani et al. (2010b), will not be described in detail: a complete discussion, including its validation, can be found in, e.g., Piani et al. (2010a) and Dosio and Paruolo (2011). Briefly, the bias adjustment is based on the calculation of a monotonically increasing transfer function (TF) such that the marginal cumulative distribution function of the adjusted variable matches that of the observations on the chosen reference period.

The observational data set EOBS (version 10) (Haylock et al., 2008) is used as reference, as it includes daily data of temperature and precipitation covering the whole European land area spatially averaged on a 0.22° grid (around 25 km). The data set has been regridded to match the resolution of the EURO-CORDEX RCMs (0.11°), which may have impacts on the tail of the adjusted precipitation distribution (see Dosio, 2016). EOBS may be affected by some potentially important limitations, such as heterogeneities (both spatial and temporal) and large absolute and relative differences over regions where dense station networks exist (e.g., Hofstra et al., 2009) or under catching in mountain areas (Lenderink, 2010). When compared to a high-density network over the Czech Republic, Kysel´y and Plavcová (2010) found that EOBS (version 2) shows large biases, especially for minimum temperature at the tail of the PDF. The issue of the heterogeneous station density and other sources of uncertainty in EOBS (version 6) is also raised by van der Schrier et al. (2013).

In order to quantify not only the European mean climatology, but also the probability of occurrence of extreme weather events, a number of climate indices from the Expert Team on Climate Change Detection and Indices (ETCCDI) (e.g., Sillmann et al., 2013) have been calculated for the present (1981–2010) and future (2071–2100) climate. Indices are listed in Table 2; the period for the calculation of the 90th and 10th reference percentile is defined as 1981–2010.

Table 2. List of ETCCDI indices

Index	**Name**	**Definition**
SM	Seasonal mean	Average over the season
TX10p	Cold days	Percentage of days where maximum daily temperature (TX) is lower than the calendar 10th percentile (centred on a 5 day window) of the reference period
TX90p	Warm days	Percentage of days where TX is higher than the calendar 90th percentile (centred on a 5 day window) of the reference period
SU	Summer days	Number of days where TX > 25◦C
ID	Ice days	Number of days where TX < 0◦C
TXx	Max TX	Maximum of daily maximum temperature in a given period (e.g. season or year)
TXn	Min TX	Minimum daily maximum temperature in a given period
WSDI	Warm spell duration	Number of days per period when, in intervals of at least six consecutive days, TX is higher than calendar 90th percentile (centred on a 5 day window) of the reference period.

TN10p	Cold nights	Percentage of days where daily minimum temperature (TN) is lower than the calendar 10th percentile (centred on a 5 day window) of the reference period
TN90p	Warm nights	Percentage of days where TN is higher than the calendar 90th percentile (centred on a 5 day window) of the reference period
FD	Frost days	Number of days where TN < 0◦C
TR	Tropical nights	Number of days where TN > 20◦C
TNx	Max TN	Maximum daily minimum temperature in a given period
TNn	Min TN	Minimum daily minimum temperature in a given period
CSDI	Cold spell duration	Number of days per period when, in intervals of at least six consecutive days, TN is lower than calendar 10th percentile (centred on a 5 day window) of the reference period.
TOTPREC	Total precipitation	Total precipitation in a given period
SDII	Simple daily intensity	Mean daily precipitation over wet days (i.e., when precipitation > 1 mm)
RR1	Number of wet days	Total number of days when precipitation >1mm
R10mm	Heavy precipitation days	Total number of days when precipitation > 10 mm
RX1day	Max 1 day precipitation	Maximum daily precipitation in a given period
CDD	Consecutive dry days	Largest number of consecutive days where precipitation <1mm
CWD	Consecutive wet days	Largest number of consecutive days where precipitation >1mm
R95ptot	Very wet days	Total precipitation in a given period when daily rainfall is larger than the 95th percentile (on wet days) of the reference period

2.3 Present-day mean climate: comparison with observations

Figure 1 shows the yearly evolution of observed (EOBS) and modelled present-day (1981-2010) summer maximum temperature (TX). Results have been area-averaged over selected sub-regions (shown in the figure). Modelled values are shown as ensemble mean of both the original and bias-adjusted RCMs.

Figure 1 shows that summer temperature is generally underestimated by most of the models across all Europe, with biases reaching up to -3° C over Scandinavia (SC), Iberian Peninsula (IP), France (FR), Middle Europe (ME), and the Alpine region (AL). Models'

variability (shown as the maximum and minimum models' values) is also very large (up to 6° C), with the coldest RCM underestimating TX up to 5° C over, e.g., IP.

After bias-adjustment results are, on average, very similar to the observations; notably, however, the extreme heat wave observed in 2003 lies outside the range of both original and bias-adjusted results over the Alps and France. In addition, the statistically significant (at 5%) trend over, e.g., Eastern Europe (EA, 0.07° C/year) is not captured by all models: only 3 runs show a significant trend close to the observed one, with values ranging between 0.06° C/year and 0.07° C/year. Crucially, bias-adjusted results are very similar to the original ones, as bias-adjustment does not alter significantly the trend.

Figure 1. Yearly evolution of present-day (1981-2010) summer maximum temperature (modified from Dosio, 2016). Observed (black), original (blue) and bias-adjusted models' results (red) are shown for each sub-domain. Units: degree K.

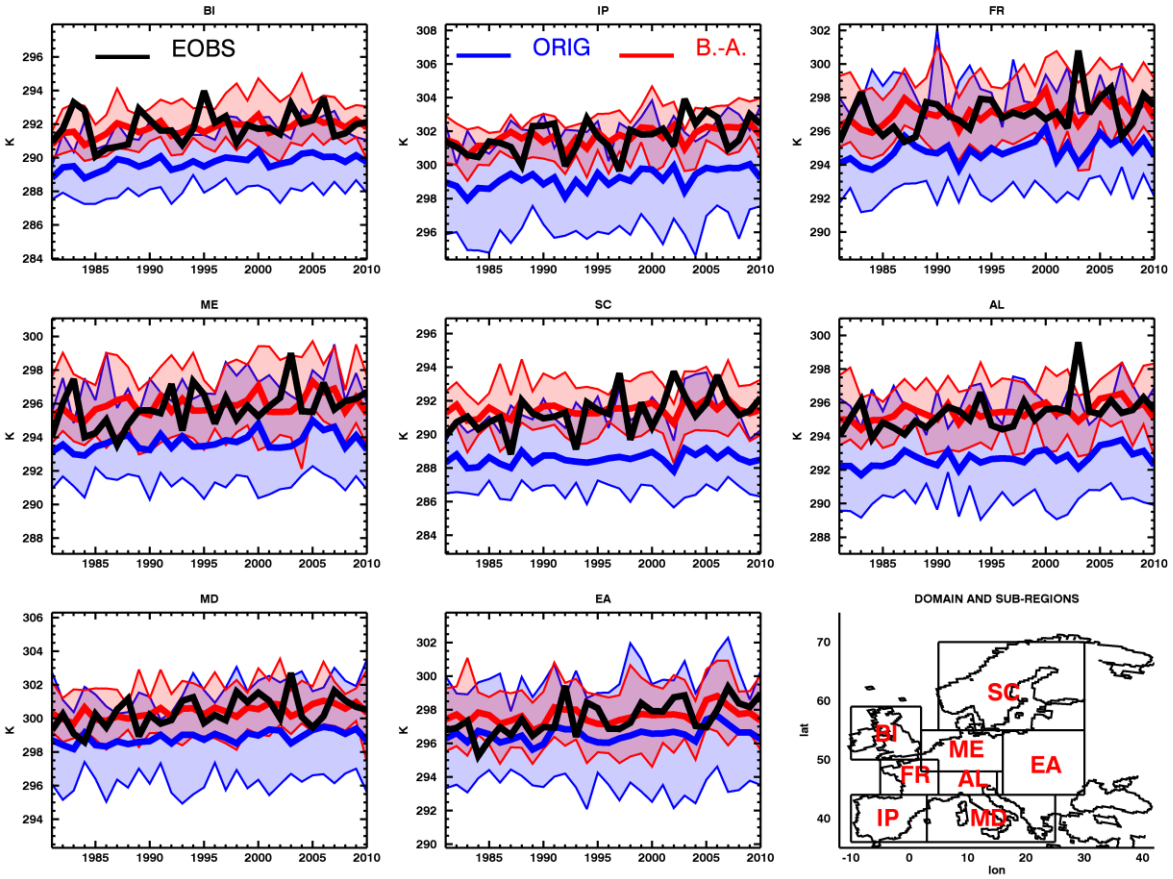

RCMs tend to generally overestimate present-climate daily rainfall, especially over the Alps, France, and Scandinavia (Figure 2), a feature that was already observed for the European Union FP6 project ENSEMBLES set of simulations (e.g., Dosio and Paruolo, 2011). In addition, it is important to note that the models' error is distributed differently across the range of precipitation intensities, with higher precipitation intensities (e.g., larger than 10 mm/d) being usually overestimated (Dosio, 2016). As expected, bias-adjusted results are closer, on average, to the observed values, although individual events, such as the high intensity precipitation over IP in 1996 may not be entirely captured.

Figure 2. Yearly evolution of present-day (1981-2010) winter total precipitation. Observed (black), original (blue) and bias-adjusted models' results (red) are shown for each sub-domain. Units: mm.

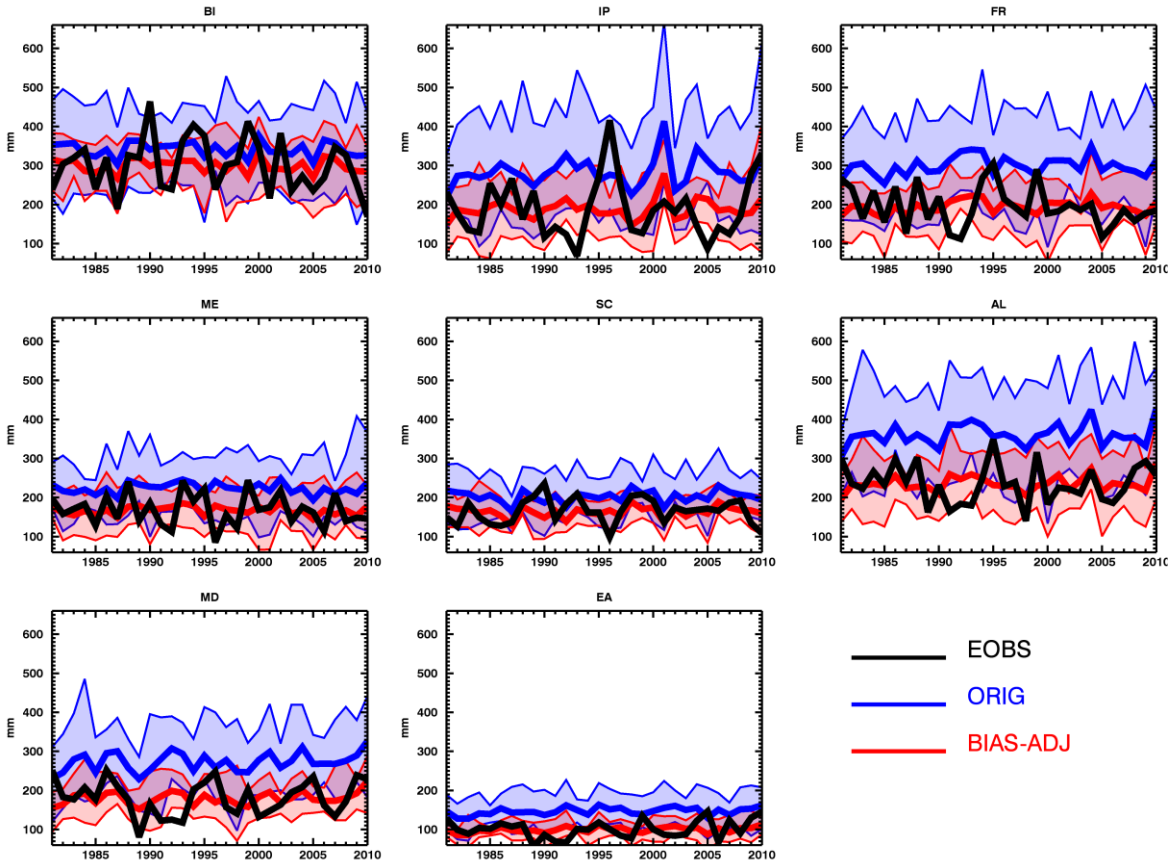

2.4 Future projections of mean climate and extreme events

Here we briefly discuss the projected change of mean temperature and precipitation, together with the change of the frequency and intensity of some extreme events that can be relevant for impact assessment studies. In addition, the effect of the bias-adjustment on the mean climate change and extreme events statistics is discussed; a complete comparison and thorough analysis of original and bias-adjusted results are reported in Dosio (2016).

2.4.1 Temperature indices

Under RCP8.5, at the end of the century, Europe is projected to face a warming of around 4° C. However, the increase temperature varis greatly both spatially and seasonally (Figure 3 and Table 3); for instance, winter T is projected to increase, on average, between 2.7° C over the British Isles (mean value of all bias-adjusted RCMs) and 5,4° C over Scandinavia, although local value may be even higher. In summer, the projected change ranges between 3.0° C over Britain and 4.7° C over the Alps and the Mediterranean regions. All models project an increase of temperature, but individual models' values can vary greatly, with differences amongst them being usually around 1° C but reaching 2.2° C for winter temperature over Eastern Europe (EA, see Table 3).

All models project a marked decrease of the number of icing days all over Europe, with the largest decrease being over Scandinavia (-25) and Eastern Europe (-20.4). A large increase in the number of summer days is projected especially over France (27) and the Alpine regions (24). However, similarly to temperature, individual models' values can largely differ.

Figure 3. Projected change of seasonal mean daily temperature for winter and summer, at the end of the century (2071-2100) compared to present day climate (1981-2010), under RCP8.5.

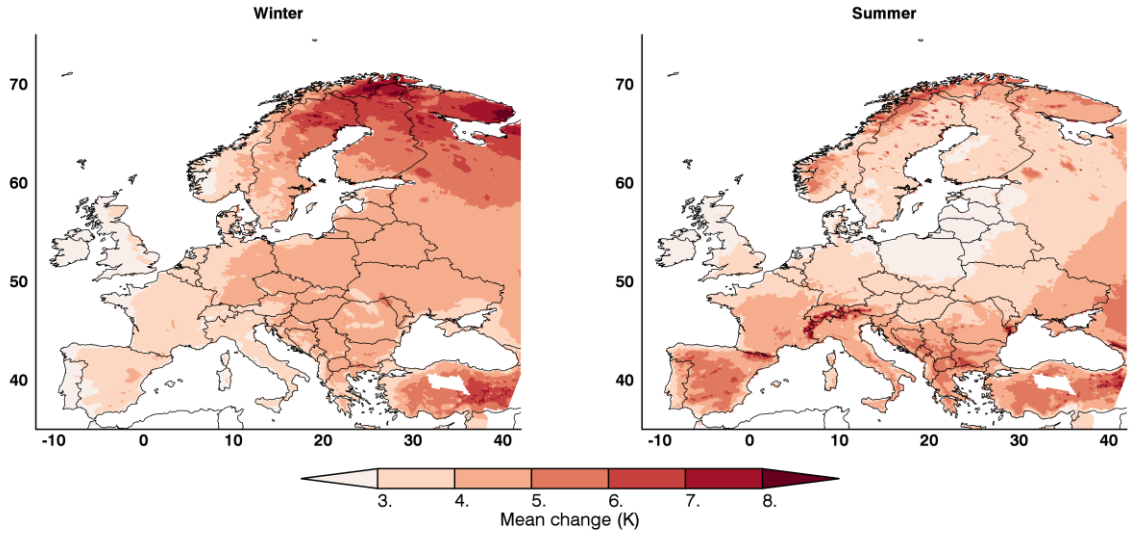

Table 3. Change of some climate indices at the end of the Century compared to present day climate under RCP8.5. Numbers indicate the models' mean, whereas minimum and maximum values are reported in brackets.

Regions	Winter mean temperature (˚ C)	Icing days	Summer mean temperature (˚ C)	Summer days
BI	2.7 (2.2,3.1)	-1.7 (-1.2,-2.3)	3.0 (2.2,3.8)	12 (6,17)
IP	2.9 (2.6,3.6)	-0.4 (-0.4,-0.6)	4.4 (3.6,5.5)	15 (13,17)
FR	3.3 (2.7,3.7)	-3.4 (-2.9,-4.0)	3.9 (2.4,5.3)	27 (15,34)
ME	3.9 (3.3,4.5)	-12.1 (-12.4,-12.1)	3.5 (2.4,4.6)	22 (13,29)
SC	5.4 (4.8,6.1)	-25.0 (-28.4,-20.8)	4.0 (3.0,5.6)	15 (8,21)
AL	3.4 (3.0,3.8)	-12.0 (-13.0,-10.9)	4.7 (3.1,6.2)	24 (16,33)
MD	3.5 (3.0,3.9)	-4.6 (-4.8,-4.4)	4.7 (3.4,6.1)	18 (16,21)
EA	4.5 (4.0,5.0)	-20.4 (-21.7,-19.4)	3.7 (2.7,4.9)	21 (17,27)
EU	4.1 (3.7,4.5)	-13.9 (-14.4,-12.3)	4.0 (3.0,5.1)	18 (14,23)

2.4.2 Effect of bias-adjustment

Figure 4 shows the comparison of the original (blue) and bias-adjusted (red) climate indices for the present period (together with the observed present day values) and for their change under RCP8.5. For each region, the index is reported for all models, together with the RCMs' median and inter-quantile range, as a measure of the uncertainty.

When comparing bias adjusted results to the original ones, we note that although the temperature change is not largely affected by bias adjustment over most areas, in some cases the difference can be substantial, such as over the Iberian Peninsula (IP) in summer and France (FR) in winter, where bias adjustment decreases (increases) the original climate change signal by nearly 1° C. Similarly, the models' uncertainty is not always reduced by bias adjustment (a part from notable exceptions like the Alps in winter) and in some cases even increased (ME in summer).

As stated previously, present-day mean TX is generally underestimated by the RCMs (Figure 1); as a consequence, the number of summer days (SU) is also underestimated by the original models, especially over central and southern Europe, where the observed SU is considerably high (Figure 4). Bias-adjustment largely corrects for these discrepancies, resulting in values of SU closer to the observed ones. However, such correction has a direct impact also on the projected change of these indices. In particular, the change of SU is largely increased by bias-adjustment over Scandinavia (SC, from 4 days/season to 15 days/season) and the British Isles (BI, from 5 days/season to 12 days/season) and reduced over southern Europe (passing from 25 days/season to 18 days/season over the Mediterranean, and from 21 days/season to 12 days/season over IP).

Similarly, bias-adjustment significantly reduces the discrepancies between observed and modelled number of icing days (ID) especially over Scandinavia and the Alps, and largely modifies the values of their projected change.

This modification, which is a consequence of the correction of the present day value, can be seen as a positive effect of bias-adjustment as compared to the original, not-adjusted projections.

Figure 4. Comparison of original and bias-adjusted maximum temperature ETCCDI indices, for all European regions. For each index, the top panel shows the value over the present period, with black circles indicating the EOBS value, and the dots the original (blue) and bias-adjusted (red) models. Horizontal lines show the RCMs' median and the vertical lines the interquantile range. The bottom panels show the climate change value of the indices under RCP8.5. DJF means winter months (December-February), whereas JJA indicate summer months (June-August) (source Dosio, 2016)

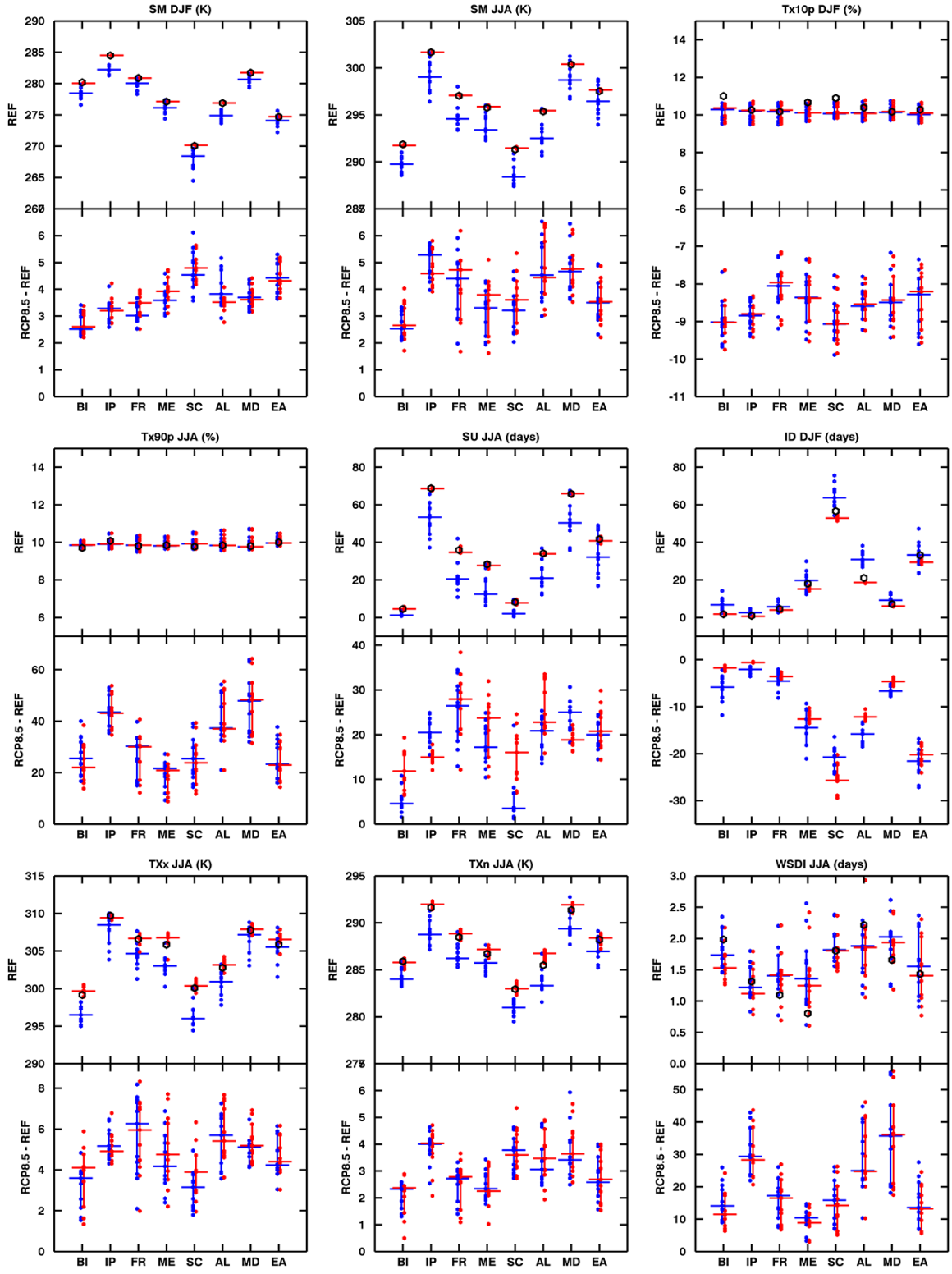

2.4.3 Precipitation indices

Projected changes of winter and summer daily precipitation are shown in Figure 5. Under RCP8.5, winter precipitation is projected to increase over most of central and northern Europe (Figure 5 and Table 4). In particular, the increase of both frequency (RR1) and intensity (SDII) (Figure 6) results in an increase of the number of consecutive wet days (CWD) and reduction of consecutive dry days (CDD). The change in precipitation frequencies distribution is not uniform, and a reduction in low precipitation intensity is accompanied by an increase of extreme events, (Table 5 and Figure 6, R10mm, RX1day, and R95ptot. See also Jacob et al., 2013) even for IP and MD, regions where total precipitation is projected to decrease.

In summer, a general reduction of precipitation is projected for all regions except Scandinavia and Eastern Europe (although the projected change over EA is very small, see Table 4); as for winter, there is a tendency toward less frequent but more severe precipitation episodes, with an increase of the number of consecutive dry days especially over Southern Europe (Table 4).

It is important to note that models do not always agree on the change of summer precipitation; although all models project a drying over the Iberian Peninsula and increased precipitation over Scandinavia, for the other regions models' results are more heterogeneous, and, sometimes, contradictory (e.g., over Middle Europe, where a mean decrease of -1.6% is the result of the large models' variability, with values ranging between -16% and +37.2% (Table 5).

Figure 5. Projected change of daily precipitation in winter and summer, at the end of the century (2071-2100) compared to present day climate (1981-2010), under RCP8.5.

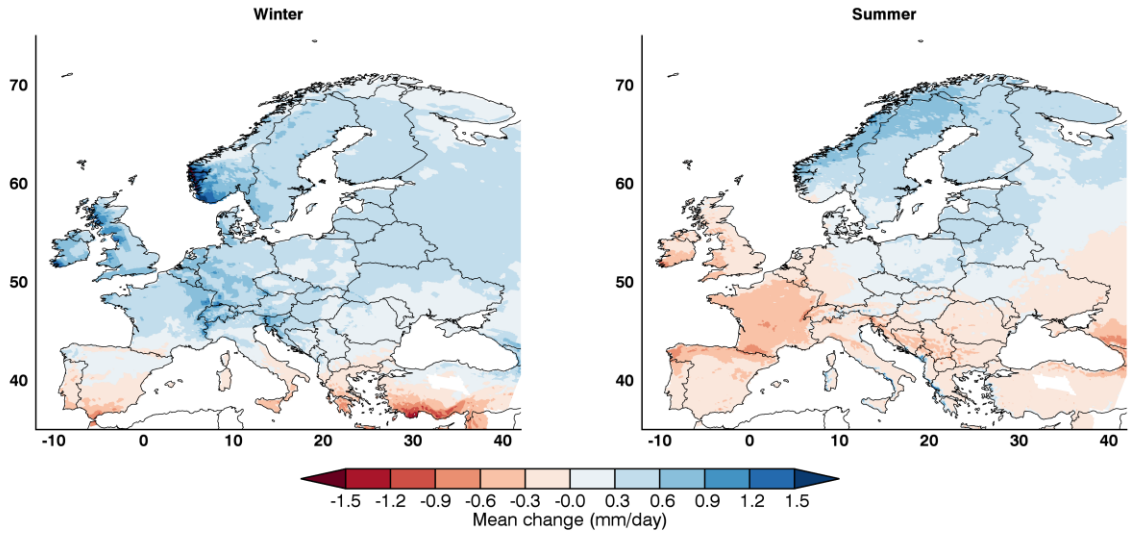

Table 4. Change of some climate indices at the end of the Century compared to present day climate under RCP8.5. Numbers indicate the models' mean, whereas minimum and maximum values are reported in brackets.

	Winter mean daily precipitation (%)	**Winter maximum daily precipitation (mm)**	**Summer mean daily precipitation (%)**	**Number of consecutive dry days in summer**
BI	19.4 (8.8,31.7)	5.1 (4.2,7.3)	-9.1 (-25.8,8.4)	2 (1,5)
IP	-3.4 (4.5,-25.9)	2.4 (-0.4,4.0)	-37.1 (-56.5,-26.5)	12 (6,14)

FR	20.5 (5.9,40.6)	5.2 (3.4,9.4)	-24.2 (-46.8,6.0)	6 (2,10)
ME	26.2 (16.4,39.1)	4.5 (3.6,6.0)	-1.6 (-16.0,37.2)	2 (0,3)
SC	25.6 (12.7,36.4)	3.9 (3.5,4.6)	17.5 (10.8,31.7)	-1 (-1,0)
AL	19.1 (9.1,24.7)	7.1 (3.6,7.0)	-6.8 (-17.8,36.0)	3 (1,4)
MD	-3.2 (-8.5,3.9)	2.8 (1.9,3.9)	-8.5 (-42.1,113.8)	8 (-4,13)
EA	24.6 (16.5,34.9)	3.7 (2.9,5.0)	3.8 (-9.4,53.9)	1 (0,1)
EU	17.0 (10.7,24.9)	4.0 (3.6,4.9)	1.6 (-7.3,37.3)	3 (1,5)

2.4.4 Effect of bias-adjustment

As discussed previously, present day precipitation is usually overestimated by the original RCMs over all areas, with bias up to 1.5 mm/day over, e.g., the Alps in DJF (Figure 2 and Figure 6). In addition, the number of wet days (RR1) is usually largely overestimated; as a consequence, total precipitation is overestimated as well.

Bias-adjusted results are relatively similar to the original ones, both in winter and summer, especially for the change in mean and total precipitation (with differences limited, usually below0.1mm/d and 10 mm/season). Results for other indices are more heterogeneous; for instance, bias-adjusted results show a smaller increase in winter of R10mm, although differences are very small (always less than 1 day/season).

Figure 6. Comparison of original and bias-adjusted winter daily precipitation ETCCDI indices, for all the European regions (source Dosio, 2016).

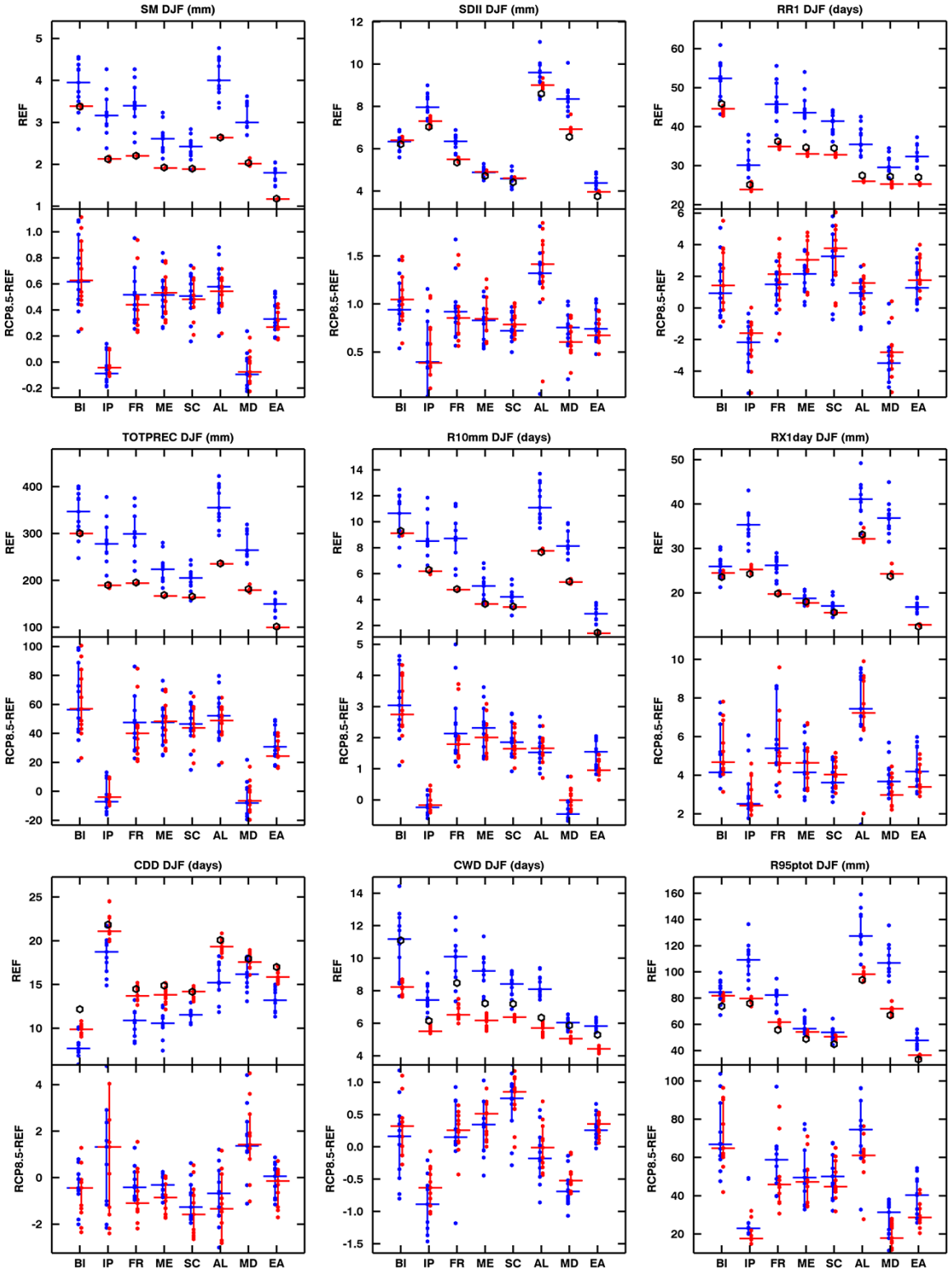

2.5 Using bias-adjusted climate change projections for impact assessment: summary and remarks

Summarizing, when climate models' projections are post-processed in order to reduce their biases over the present climate, the resulting climate change may also be altered. This effect has to be taken into account when using bas-adjusted climate projections for the assessment on climate change on specific sectors. Some main considerations are listed below:

1. The fact that bias adjustment affects the change of mean climate is known and still much debated by the scientific community: whereas some authors like Gobiet et al. (2015) claim that the bias adjustment improves the climate change signal, as this modification is caused by the removal of the intensity-dependent errors in the original models, others, such as Cannon et al. (2015), prefer the use of modified quantile mapping designed to explicitly preserve relative changes in simulated (precipitation) quantiles. Finally, Maurer and Pierce (2014) claim that bias adjustment has no overwhelming negative or positive effect on precipitation changes, and there is no clear advantage in using a trend-preserving bias adjustment.

Inter-model variability is also affected by bias adjustment, although by a less extent; in their analysis, Gobiet et al. (2015) show that the intensity-dependent model error is partly responsible for the model uncertainty in the climate change signal; as for the main signal, the reduction of these intensity-dependent biases may lead to an improved (i.e., reduced) model uncertainty. However, this is not always the case, and the increase in the inter-model variability due to bias adjustment requires further investigation.

2. Percentile-based indices (such as Tx90p) are robust to bias adjustment: this result emphasizes the claim by many authors (e.g., Alexander et al., 2006) of the superiority of these indices compared to fixed-threshold ones, especially for the analysis of the change of climate extremes on, e.g., different regions.

3. Impact assessment on specific sectors (e.g., agriculture and infrastructure), however, still requires projections of threshold-based indices (such as SU or ID), which are generally poorly simulated by the original RCMs over the present climate, as such that even the projected climate change may not be realistic or reliable (Dosio, 2016). For threshold-based indices, we argue that bias adjustment can provide not only a substantial improvement of the absolute present climate values but also a more robust climate change signal.

4. Finally, bias adjustment cannot alter the time dependence of the original distribution; consequently, the skill of the model in simulating indices related to the duration of an event (e.g., WSDI or CDD) will not be necessarily improved.

In conclusion, it is important to understand that bias adjustment will not correct for models' deficiencies in representing fundamental physical processes, and the projections of these models will remain unreliable, even after bias adjustment.

3 Models' runs selection

A set of 12 RCMs' bias-adjusted climate change projections is provided for use by the PESETA III impact models; such a large ensemble of runs is essential to quantify the uncertainty in future climate projections (the so-called inter-model variability). In fact, each model's run (driven by the same emission scenario) represents an equally plausible projection of the future evolution of the climate. However, due to differences in the models' formulation and physical parameterization, the climate change signal projected by different models may present significant differences.

The PESETA III protocol requires that, from the original, large ensemble of bias-adjusted runs, a smaller sub-set of core runs (5) is selected to be run by all impact models. The sub-set of core runs needs to be able to reproduce, as accurately as possible, the inter-model variability in the future projections of the entire ensemble.

This selection has been performed by means of Principal Component Analysis (PCA), a statistical technique that converts a set of possibly correlated variables into a smaller set of linearly uncorrelated variables called principal components (PCs). This transformation is defined in such a way that the first principal component has the largest possible variance (that is, accounts for as much of the variability in the data as possible). The coefficients of the transformation are called loadings, and describe the weight by which each (standardized) original variable should be multiplied to get the transformed one (Mendlik and Gobiet, 2016, Maule and Christensen, 2015).

Figure 7. Value of the loadings for the first 4 PCs (PC0-PC3). Each loading is shown for each ETCCDI index, region, and season, namely winter (DJF) and summer (JAS).

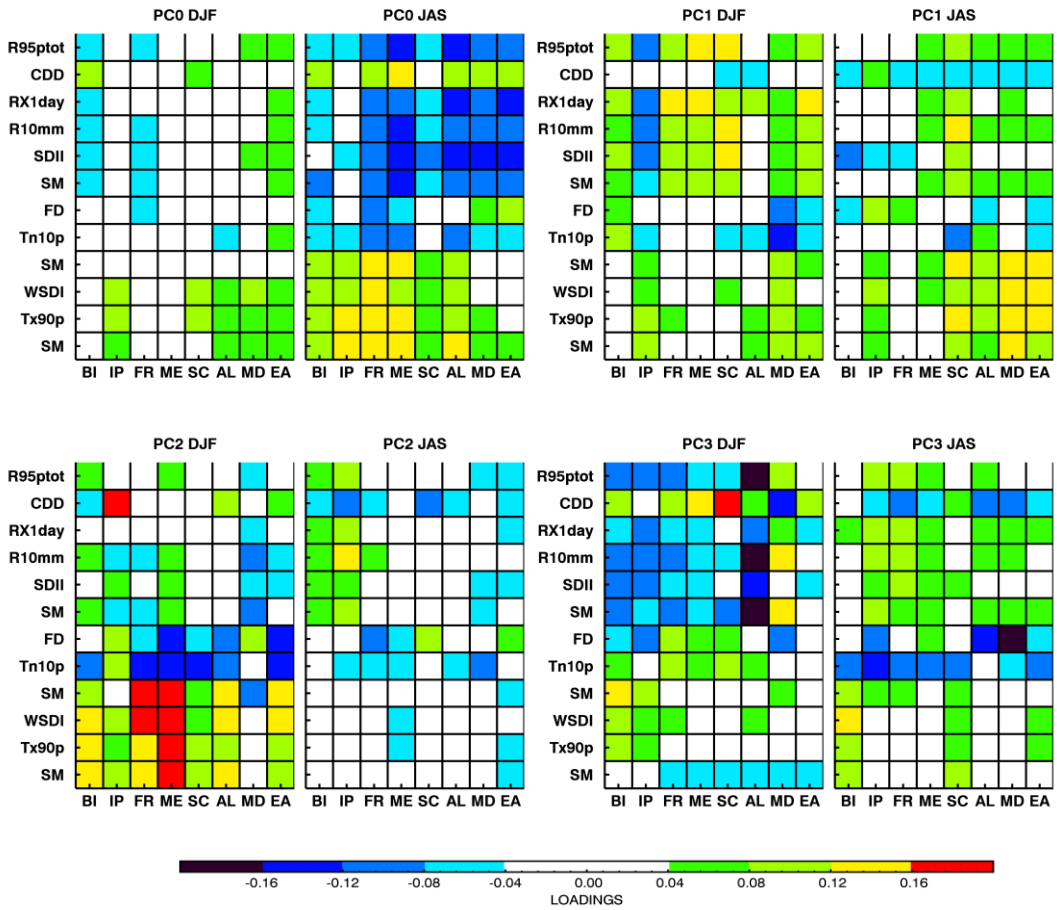

In our case, for each RCM, the PCA was calculated by using the climate change signal of 12 ETCCDI indices, for both seasonal mean (TX, TN and precipitation) and extremes (TX90p, WSDI, TN10p, FD, SDII, CDD, R10mm, RX1day, R95ptot) over the 8 sub-regions

in both winter and summer. By plotting the loadings for each index, region, and season (Figure 7) it can be noted that, for instance, the first PC (PC0) is mostly related to the variance of summer precipitation and temperature (mean and extreme), whereas PC2 mostly accounts for the variance of winter temperature.

It is also important to note that the first two PCs alone explain more that 50% of the total variance, whereas by using 4 PCs the total amount of variance explained is more than 80% (Figure 8). By plotting the PCA results of each RCM in the PCs' space it is possible to visually select the RCMs that maximize the inter-model variability, for each pair of PCs. As an example, for the first two components, PC0 and PC1, it is evident that e.g. model R1-G1 and model R5-G5 have an opposite behaviour, whereas for the pair PC2-PC3 model R1-G2 is mostly neutral (figure 8).

Figure 8. Total variance explained by each PCs (top panel), and plots of the climate change signal of each RCM in the PC space, for different pairs of PCs. RCMs are grouped using different colours according to the driving GCM.

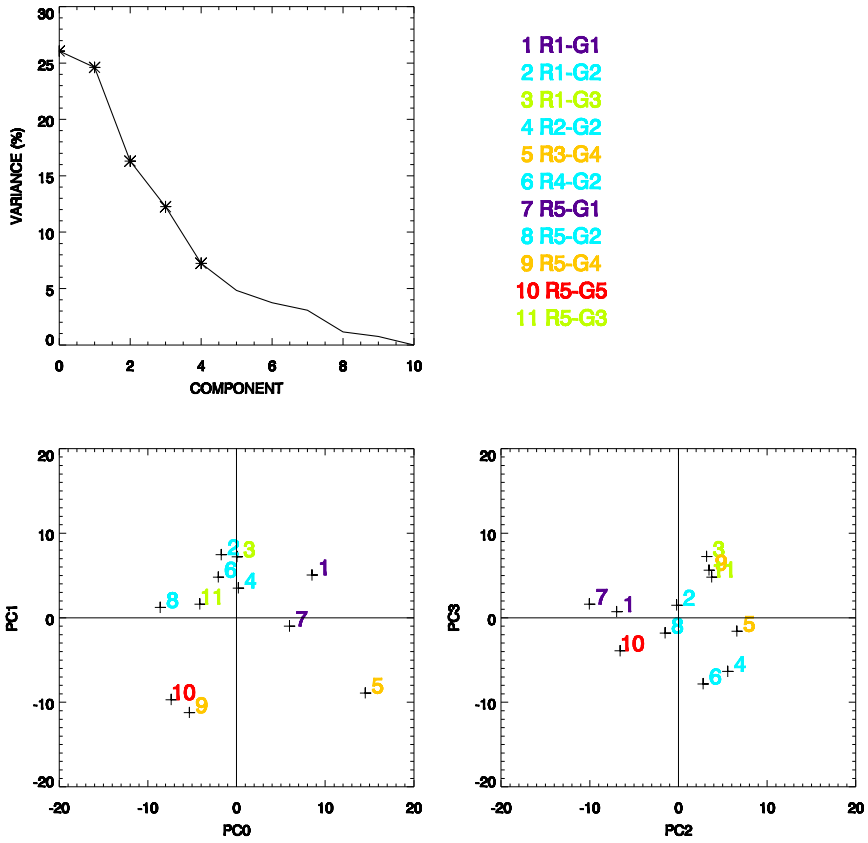

From this analysis, the following sub-set of runs can be chosen:

- **R1-G1:** CNRM-CERFACS-CNRM-CM5_r1i1p1_CLMcom-CCLM4-8-17
- **R1-G2:** ICHEC-EC-EARTH_r12i1p1_CLMcom-CCLM4-8-17
- **R3-G4:** IPSL-IPSL-CM5A-MR_r1i1p1_IPSL-INERIS-WRF331F
- **R5-G5:** MOHC-HadGEM2-ES_r1i1p1_SMHI-RCA4
- **R5-G3:** MPI-M-MPI-ESM-LR_r1i1p1_SMHI-RCA4

This selection, although subjective, reflects the spread of the total RCMs' ensemble in the various PCs' spaces; in addition, the five core runs have been chosen so that RCMs are driven by 5 different GCMs (considering IPSL-CM5A different from CNRM-CERFACS-CM5).

R1-G2 (ICHEC-EC-EARTH_r12i1p1_CLMcom-CCLM4-8-17) may be regarded as an 'average' model, especially for temperature related indices. However, this 'average' model shows a climate change signal for precipitation indices that is usually drier than the other models (at least for mean precipitation). However, choosing a model that is perfectly 'average' on every index, season and region is not possible.

To validate the choice of the core runs, Figure 9 shows the climate change signal of the indices for every model on every region, in winter. Red symbols represent the core RCMs, black symbols the other RCMs of the complete ensemble, and the blue one the 'average' model. Although differences exist depending on the region, season, and index, it can be seen that generally the spread of the selected core runs accounts for most of the total inter-model variability.

Figure 9. Climate change signal of the ETCCDI indices used in the PCA analysis, for all sub-regions, in winter. For each index, and region, each symbol represents a RCM. Red symbols represent the 5 core runs, with the blue one the "average" model run. First row shows TX indices, second row the TN ones, and the bottom two rows the precipitation indices.

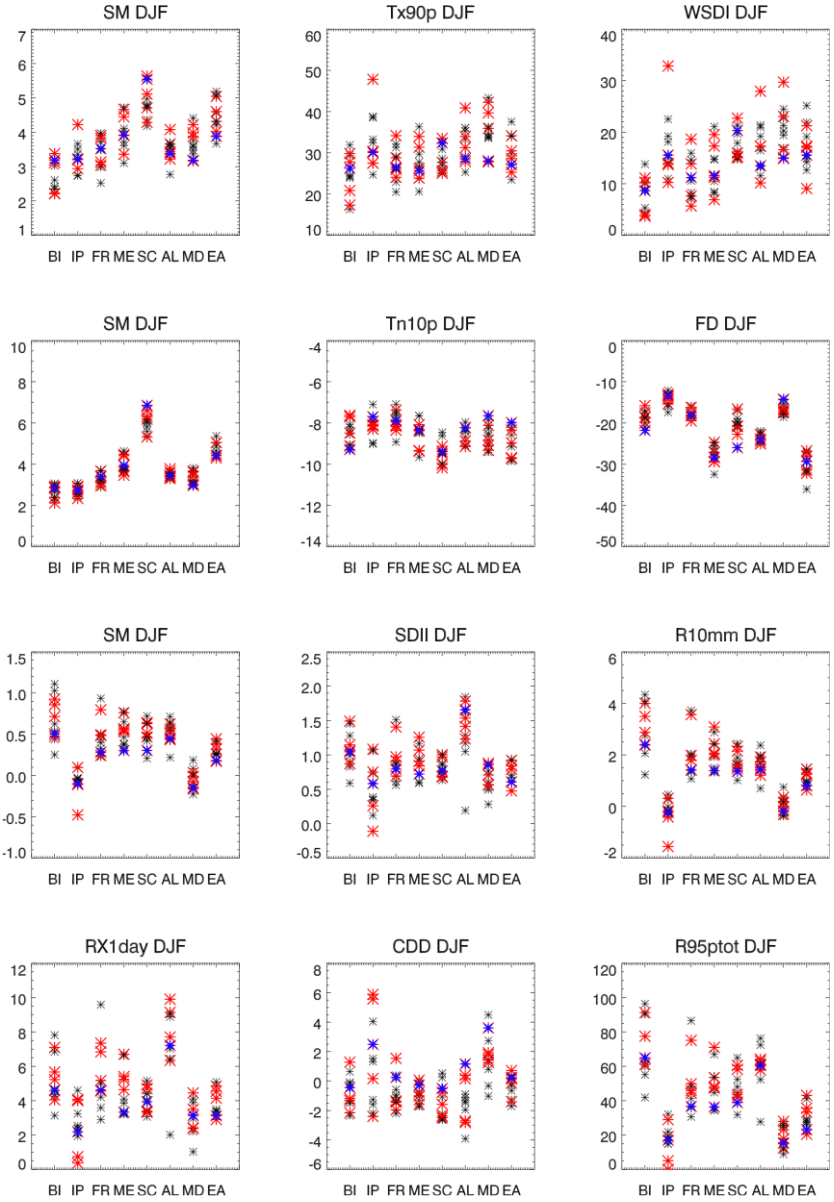

4 Time of reaching 2°C warming

Finally, the PESETA II protocol requires investigating the impacts of a 2°C global warming, compared to the preindustrial period. As, for PESETA III, climate projections are forced by the RCP8.5 emission scenario, a 2°C warming may be reached, depending on the model run, before the end of the century. To define the timing of reaching the 2°C warming, we follow the same procedure used in the FP7 project IMPACT2C (http://impact2c.hzg.de), where:

- It is assumed that the climate in a +2°C world is comparable irrespective of when and how fast this warming is reached
- An RCM is defined to project a 2°C global warming when the corresponding driving GCM reaches the 2°C threshold, under RCP8.5 emission scenario
- For each GCM-RCM run, the +2°C period is defined as the 30 year period centered around the year when the 2°C global warming is first reached

The list of 2°C period, for each model run, is reported in table 6. Few considerations have to be made:

- For the ICHEC-EC-EARTH GCM (G2) three different realizations are used by different RCMs (r1i1p1, r3i1p1m, r12i1p1); as a consequence, the timing of reaching +2°C for e.g. R2-G2 is different than for R4-G2
- Since some RCMs are driven by the same GCM (e.g., R1-G3 and R5-G3), in this case the timing of reaching +2°C is the same.
- However, even in the case above, the climate projected over Europe by the two GCM-RCMs may be substantially different, as the RCM can alter the information inherited by the driving GCM.
- the underlying assumption that 2 degrees of global warming would give the same climate change, no matter the speed with which this warming is reached, would require special care for time dependent phenomena, such as mean sea level rise or carbon stock in the forests, which respond not only to the change in temperature but also to the cumulated time when it is reached.

Table 6. List of runs and corresponding 30 year period when a 2°C global warming is reached (compared to preindustrial period). Core runs are highlighted in bold

Acronym	Central year	Period of 2°C global warming
R1-G1	**2044**	**2030-2059**
R1-G2	**2041**	**2027-2056**
R1-G3	2044	2030-2059
R2-G2	2043	2029-2058
R3-G4	**2035**	**2021 2050**
R4-G2	2042	2028-2057
R5-G1	2044	2030-2059
R5-G2	2041	2027-2056
R5-G4	2035	2021-2050
R5-G5	**2030**	**2016-2045**
R5-G3	**2044**	**2030-2059**

5 Conclusions

A methodology has been described to provide PESETA III impact modellers with high resolution, bias-adjusted projections of climate change for Europe under RC8.5. Three main topics have been discussed:

1) the bias-adjustment technique and its effect of a the mean climate change signal and indices of extreme events, which are relevant for impact assessment on different sectors
2) a methodology based on Principal Component Analysis (PCA) to select a subset of models' runs to be used as core runs (i.e. compulsory to all participant impact groups) in PESTEA III
3) a methodology to identify the timing of reaching a 2°C global warming compared to preindustrial period, to investigate the impact, at European level, of a +2°C world.

Finally, some general remarks, together with suggestions for future work, are presented:

First, it is important to understand that the reliability of any climate projection based on bias-adjusted results greatly depends on the observational data set used as reference; for instance, in case of a mismatch between the resolution of models and observations, the effect on the PDF (and, as a consequence, the value of the climate indices) may be relevant. As high-resolution climate projections are becoming more and more frequent, with convection-scale (5 Km or less) runs expected to be available in the near future, the availability of a high-resolution, spatially and temporally homogeneous observational data set becomes of fundamental importance.

Even though the E-OBS dataset has been extensively used inside as reference high-resolution observational dataset for Europe, it is affected by some potentially important limitations, such as heterogeneities (both spatial and temporal) and large absolute and relative differences over different regions. Regional high-resolution, station based, public databases exist for e.g., the Alpine area and Spain but they are yet to be integrated in a single homogeneous European-wide dataset.

Moreover, as some impact models need a large set of meteorological variables, besides temperature and precipitation, such as wind speed, solar radiation or relative humidity it is of great importance to investigate the feasibility of bias-adjusting these variables preserving, at the same time, the temporal day by day correlation with e.g. temperature.

References

Alexander, L. V., et al. (2006), Global observed changes in daily climate extremes of temperature and precipitation, *J. Geophys. Res.*, doi:10.1029/2005JD006290.

Boberg, F., and J. H. Christensen (2012), Overestimation of Mediterranean summer temperature projections due to model deficiencies, *Nat. Clim. Change*, *2*(4), 433–436, doi:10.1038/nclimate1454.

Cannon, A. J., S. R. Sobie, and T. Q. Murdock (2015), Bias correction of GCM precipitation by quantile mapping: How well do methods preserve changes in quantiles and extremes?, *J. Clim.*, *28*(17), 6938–6959, doi:10.1175/JCLI-D-14-00754.1.

Dosio, A., and P. Paruolo (2011), Bias correction of the ENSEMBLES high-resolution climate change projections for use by impact models: Evaluation on the present climate, *J. Geophys. Res.*, *116*, D16106, doi:10.1029/2011JD015934.

Dosio, A., P. Paruolo, and R. Rojas (2012), Bias correction of the ENSEMBLES high resolution climate change projections for use by impact models: Analysis of the climate change signal, *J. Geophys. Res.*, *117*, D17110, doi:10.1029/2012JD017968.

Dosio A. (2016): Projections of climate change indices of temperature and precipitation from an ensemble of bias-adjusted high-resolution EURO-CORDEX regional climate models, *Journal of Geophysical Research D: Atmospheres,* DOI: 10.1002/2015JD024411

Ehret, U., E. Zehe, V. Wulfmeyer, K. Warrach-Sagi, and J. Liebert (2012), HESS Opinions "Should we apply bias correction to global and regional climate model data?", *Hydrol. Earth Syst. Sci.*, *16*(9), 3391–3404, doi:10.5194/hess-16-3391-2012.

Fowler, H. J., S. Blenkinsop, and C. Tebaldi (2007), Linking climate change modelling to impacts studies: Recent advances in downscaling techniques for hydrological modelling, *Int. J. Climatol.*, *27*(12), 1547–1578.

Gabaldón-Leal, C., I. Lorite, M. Mínguez, J. Lizaso, A. Dosio, E. Sanchez, and M. Ruiz-Ramos (2015), Strategies for adapting maize to climate change and extreme temperatures in Andalusia, Spain, *Clim. Res.*, *65*, 159–173, doi:10.3354/cr01311.

Gobiet, A., M. Suklitsch, and G. Heinrich (2015), The effect of empirical-statistical correction of intensity-dependent model errors on the climate change signal, *Hydrol. Earth Syst. Sci. Discuss.*, *12*, 5671–5701, doi:10.5194/hessd-12-5671-2015.

Jacob, D., et al. (2013), EURO-CORDEX: New high-resolution climate change projections for European impact research, *Reg. Environ. Change*, *14*, 563–578, doi:10.1007/s10113-013-0499-2.

Haylock, M. R., N. Hofstra, A. M. G. Klein Tank, E. J. Klok, P. D. Jones, and M. New (2008), A European daily high-resolution gridded data set of surface temperature and precipitation for 1950-2006, *J. Geophys. Res.*, *113*, D20119, doi:10.1029/2008JD010201.

Kysel´y, J., and E. Plavcová (2010), A critical remark on the applicability of EOBS European gridded temperature data set for validating control climate simulations, *J. Geophys. Res.*, *115*, D23118, doi:10.1029/2010JD014123.

Lenderink, G. (2010), Exploring metrics of extreme daily precipitation in a large ensemble of regional climate model simulations, *Clim. Res.*, doi:10.3354/cr00946.

Li, H., J. Sheffield, and E. F. Wood (2010), Bias correction of monthly precipitation and temperature fields from Intergovernmental Panel on Climate Change AR4 models using equidistant quantile matching, *J. Geophys. Res.*, doi:10.1029/2009JD012882.

Maule, C. F., and O. B. Christensen (2015), Improving the capacity of agro-meteorological crop modelling to integrate climatic variability and extreme weather events, MODEXTREME D3.3 deliverable report, 31 pp.

Maurer, E. P., and D. W. Pierce (2014), Bias correction can modify climate model simulated precipitation changes without adverse effect on the ensemble mean, *Hydrol. Earth Syst. Sci.*, *18*(3), 915–925, doi:10.5194/hess-18-915-2014.

Mbaye, M. L., A. Haensler, S. Hagemann, A. T. Gaye, C. Moseley, and A. Afouda (2015), Impact of statistical bias correction on the projected climate change signals of the regional climate model REMO over the Senegal River Basin,

Mendlik T. and Gobiet A., (2016), Selecting climate simulations for impact studies based on multivariate patterns of climate change, *Climatic Change* (2016) 135:381–393 DOI 10.1007/s10584-015-1582-0

Migliavacca, M., et al. (2013), Modeling burned area in Europe with the community land model, *J. Geophys. Res. Biogeosci*, *118*, 265–279, doi:10.1002/jgrg.20026.

Piani, C., J. O. Haerter, and E. Coppola (2010a), Statistical bias correction for daily precipitation in regional climate models over Europe, *Theor. Appl. Climatol.*, *99*(1–2), 187–192, doi:10.1007/s00704-009-0134-9.

Piani, C., G. P. Weedon, M. Best, S. M. Gomes, P. Viterbo, S. Hagemann, and J. O. Haerter (2010b), Statistical bias correction of global simulated daily precipitation and temperature for the application of hydrological models, *J. Hydrol.*, *395*(3–4), 199–215, doi:10.1016/j.jhydrol.2010.10.024.

Ruiz-Ramos, M., A. Rodríguez, A. Dosio, C. M. Goodess, C. Harpham, M. I. Mínguez, and E. Sánchez (2015), Comparing correction methods of RCM outputs for improving crop impact projections in the Iberian Peninsula for 21st century, *Clim. Change*, *134*, 283–297, doi:10.1007/s10584-015-1518-8.

Rojas, R., L. Feyen, A. Dosio, and D. Bavera (2011), Improving pan-European hydrological simulation of extreme events through statistical bias correction of RCM-driven climate simulations, *Hydrol. Earth Syst. Sci.*, *15*(8), 2599–2620, doi:10.5194/hess-15-2599-2011.

Russo, S., A. Dosio, A. Sterl, P. Barbosa, and J. Vogt (2013), Projection of occurrence of extreme dry-wet years and seasons in Europe with stationary and nonstationary Standardized Precipitation Indices, *J. Geophys. Res. Atmos.*, *118*, 7629–7639, doi:10.1002/jgrd.50571.

Sillmann, J., V. V. Kharin, F. W. Zwiers, X. Zhang, and D. Bronaugh (2013), Climate extremes indices in the CMIP5 multimodel ensemble: Part 2. Future climate projections, *J. Geophys. Res. Atmos.*, *118*, 2473–2493, doi:10.1002/jgrd.50188.

Taylor, K. E., R. J. Stouffer, and M. Ga (2012), An overview of CMIP5 and the experiment design, *Bull. Am. Meteorol. Soc.*, *93*(4), 485–498, doi:10.1175/BAMS-D-11-00094.1.

Themeßl, M. J., A. Gobiet, and G. Heinrich (2011), Empirical-statistical downscaling and error correction of regional climate models and its impact on the climate change signal, *Clim. Change*, *112*, 449–468, doi:10.1007/s10584-011-0224-4.

Thrasher, B., E. P. Maurer, C. McKellar, and P. B. Duffy (2012), Technical note: Bias correcting climate model simulated daily temperature extremes with quantile mapping, *Hydrol. Earth Syst. Sci.*, *16*(9), 3309–3314, doi:10.5194/hess-16-3309-2012.

Vuuren, D. P., et al. (2011), The Representative Concentration Pathways: An overview, *Clim. Change*, *109*(1–2), 5–31, doi:10.1007/s10584-011-0148-z.

List of figures

List of tables

No table of figures entries found.

Europe Direct is a service to help you find answers to your questions about the European Union.

Freephone number (*)**:**

00 800 6 7 8 9 10 11

(*) The information given is free, as are most calls (though some operators, phone boxes or hotels may charge you).

More information on the European Union is available on the internet (http://europa.eu).

HOW TO OBTAIN EU PUBLICATIONS

Free publications:

- one copy:
  via EU Bookshop (http://bookshop.europa.eu);
- more than one copy or posters/maps:
  from the European Union's representations (http://ec.europa.eu/represent_en.htm);
  from the delegations in non-EU countries (http://eeas.europa.eu/delegations/index_en.htm);
  by contacting the Europe Direct service (http://europa.eu/europedirect/index_en.htm) or
  calling 00 800 6 7 8 9 10 11 (freephone number from anywhere in the EU) (*).

  (*) The information given is free, as are most calls (though some operators, phone boxes or hotels may charge you).

Priced publications:

- via EU Bookshop (http://bookshop.europa.eu).

KJ-NA-29444-EN-N

JRC Mission

As the science and knowledge service of the European Commission, the Joint Research Centre's mission is to support EU policies with independent evidence throughout the whole policy cycle.

EU Science Hub
ec.europa.eu/jrc

@EU_ScienceHub

EU Science Hub - Joint Research Centre

Joint Research Centre

EU Science Hub

doi:10.2760/44883
ISBN 978-92-79-97261-4

Publications Office